

## Nanoscopic hybrid systems with a polarity-controlled gate-like scaffolding for the colorimetric sensing of long-chain carboxylates.

Carmen Coll, Rosa Casasús, Elena Aznar, M. Dolores Marcos, Ramón Martínez-Máñez, Félix Sancenón, Juan Soto, and Pedro Amorós

### Chemicals

The products tetraethylorthosilicate (TEOS), *n*-cetyltrimethylammonium bromide (CTAB), sodium hydroxide (NaOH), triethanolamine (TEAH<sub>3</sub>), tris(2,2'-bipyridyl)ruthenium(II) chloride hexahydrate (Ru(bipy)<sub>3</sub>Cl<sub>2</sub>·6H<sub>2</sub>O), and all the carboxylates used in the manuscript were provided by Aldrich and used as received.

### Synthesis of the mesoporous support (MCM41-type material).

The synthesis of the MCM41-type mesoporous support was carried out following the so-called "atranane route", a simple preparative technique based on the use of complexes that include triethanolamine (TEAH<sub>3</sub>) related ligands (i.e. in general "atranes" and silatranes for the silicon-containing complexes) as hydrolytic inorganic precursors and surfactants as porogen species. The molar ratio of the reagents in the mother liquor was fixed to 8 TEAH<sub>3</sub>: 2 TEOS: 0.52 CTAB: 0.5 NaOH: 180 H<sub>2</sub>O. In a typical synthesis leading to the MCM-41 pure silica, 4,23 g of CTAB (cetyltrimethylammonium bromide) were added at 60 °C to a solution of TEAH<sub>3</sub> (23 mL) containing 0.012 mol of NaOH and 0,045 mol of a silatrane derivative of TEAH<sub>3</sub> (e.g. in the form of Si(TEA)(TEAH<sub>2</sub>), where TEA is the fully deprotonated ligand). Then, 180 mL of deionized water were slowly added with vigorous stirring at 50 °C. After few minutes, a white suspension resulted. This mixture was aged at room temperature overnight. The resulting powder was collected by filtration, washed with water and ethanol. Finally the solid was dried at 70 °C (**MCM-41 as-synthesized**). To prepare the final porous material (**MCM-41**), the as-synthesised solid was calcined at 550 °C using oxidant atmosphere for 5h in order to remove the template phase.

### Synthesis of the imidazolium derivative *N*-methyl-*N*'-propyltrimethoxysilylimidazolium chloride (**1**).

The *N*-methyl-*N*'-propyltrimethoxysilylimidazolium chloride was prepared as follows (Valkenberg, M.H; Hölderich, W.F; de Castro, C, *Top. Catal* **2000**, *14*,139) A mixture of *N*-methyl-*N*'-propyltrimidazole (6.57g, 80 mmol) and 3-(chloropropyl)trimethoxysilane (15.89 g, 80 mmol) were stirred in a dry 100 ml flask under nitrogen flow at 95 °C for 24 h. After cooling at room temperature, the resulting liquid product was extracted with ether. The final compound was obtained as a yellow liquid.

### Synthesis of the imidazolium-functionalised dye-containing material (**MS-Im**).

1.0 g of templated-free **MCM-41** was suspended in 30 ml of anhydrous acetonitrile and heated at 110° C in a Dean-Stark in order to remove the adsorbed water by azeotropic distillation under inert atmosphere (Ar gas). Then the dye tris(2,2'-bipyridyl)ruthenium(II) chloride (0.6 g, 0.8 mmol) was added to the suspension at room temperature and stirred for 24 hours with the aim of loading the pores of the **MCM-41** scaffolding. After this, an excess of *N*-methyl-*N*'-propyltriethoxysilylimidazolium chloride (**1**) was added and the suspension was stirred for 5.5 hours. Following this grafting procedure a significant fraction of the imidazolium groups will be preferentially attached to the pore outlets; i.e the functionalization would take place more easily on the external surface than inside the channels which are filled with the

Ru(bipy)<sub>3</sub><sup>2+</sup> dye. The final orange solid (**MS-Im**) was filtered, washed with acetonitrile and dried at 70 °C for 12 hours.

For the sake of comparison, and as a control solid, a similar material was prepared using as support a non-mesoporous silica (fumed silica). The procedure was the same as described in the paragraph above but using in this case 1.0 g of fumed silica. The final pale orange solid (**FS-Im**) was filtered, washed with acetonitrile and dried at 70 °C for 12 hours. The **FS-Im** solid consists of a “flat” surface (i.e. without the presence of nanoscopic pores) with anchored imidazolium groups and a certain amount of adsorbed Ru(bipy)<sub>3</sub><sup>2+</sup> dye.

### **General Techniques**

XRD, TG analysis, IR spectroscopy, elemental analysis, EDX microscopy, N<sub>2</sub> adsorption-desorption, UV-visible spectrophotometer techniques were employed to characterize the materials. X-ray measurements were performed on a Seifert 3000TT diffractometer using Cu K $\alpha$  radiation. Thermo-gravimetric analysis were carried out on a TGA/SDTA 851e Mettler Toledo balance, using an oxidant atmosphere (Air, 80 mL/min) with a heating program consisting on a heating ramp of 10 °C per minute from 393 K to 1273 K and an isothermal heating step at this temperature during 30 minutes. IR spectra were recorded on a Jasco FT/IR-460 Plus between 400 and 4000 (cm<sup>-1</sup>) diluting the solids in KBr pellets. N<sub>2</sub> adsorption-desorption isotherms were recorded on a Micromeritics ASAP2010 automated sorption analyser. The samples were degassed at 120°C in vacuum overnight. The specific surfaces areas were calculated from the adsorption data in the low pressures range using the BET model. Pore sized was determined following the BJH method. UV-visible spectroscopy was carried out with a Lambda 35 UV/Vis Spectrometer Perkin Elmer Instruments.

The thermal analysis of the **MS-Im** solid shows typical behaviour in functionalised mesoporous materials; i.e. a first weight loss between 25 and 150°C related to the solvent evolution, a second step, between 150 and 500 °C due to the combustion of the organics and a final loss in the 500 - 1000 °C range related to the condensation of the silanol groups.

The infrared spectrum of **MS-Im** and that of the **MCM-41** support show dominant bands due to the silica matrix (1250, 1087,802 and 462 cm<sup>-1</sup>) and those related to the vibrations of water molecules (3420 and 1620 cm<sup>-1</sup>). Apart from that, regarding the dye loading and functionalization process, small bands related to the organic moieties (bipyridine and imidazolium) in **MS-Im** were observed compared to the initial **MCM-41** calcined material. The most remarkable bands are found at 2900 cm<sup>-1</sup> in **MS-Im** and due to C-H stretching vibrations.

Several **MS-Im** materials were prepared and their content in imidazolium groups and ruthenium(II) dye were determined from elemental analysis, thermal analysis and X-ray microanalysis. From the different prepared solids a value ranging from 6 to 9 wt% of imidazolium and a value ranging from 14 to 17 wt% of Ru(bipy)<sub>3</sub><sup>2+</sup> were obtained. Despite these variation in imidazolium and ruthenium(II) dye contents in different synthesis all the solids prepared display similar sensing features.

The N<sub>2</sub> adsorption-desorption isotherms of the **MCM-41** calcined material shows a typical curve for these mesoporous solids; i.e. an adsorption step at intermediate  $P/P_0$  value (0.3). This curve corresponds to a type IV isotherm, in which the observed step can be related to the nitrogen condensation inside the mesopores by capillarity. The absence of a hysteresis loop in this interval and the narrow pore distribution suggest the existence of uniform cylindrical mesopores (2.50 nm, 0.65 cm<sup>3</sup>·g<sup>-1</sup>). The application of the BET model resulted in a value for the total specific surface of 1025.4 m<sup>2</sup>/g. From the value of the XRD  $a_0$  cell parameter (45.31 Å) and the pore diameter (2.50 nm), a value for the wall thickness of 20 Å can be calculated.

### **Imidazolium-carboxylate interaction**

An interesting question related with this system is the evaluation of the imidazolium-carboxylate interaction. This is an important issue and some experiments have been carried out

to address this point. When an excess of a certain carboxylate is added to solid **MS-Im**, the elemental and thermogravimetric analysis clearly show an increase of the organic material indicating that a self-assembly of the corresponding carboxylate on the imidazolium surface occurs. However, it was rather difficult to obtain reliable quantitative results when compared both thermogravimetric and elemental analysis. As a possible cause of error we might hint the presence of the  $\text{Ru}(\text{bipy})_3^{2+}$  dye at the pores that is partially delivered even at low reaction times in the presence of certain carboxylates. Moreover, typically for MCM41-type solids, below 300 °C water loss due to an undetermined number of silanol groups condensation is observed making the quantitative interpretation rather complex. Because of that problem we opted for to use a simpler solid support in order to carry out studies on the imidazolium-carboxylate interactions. Thus, in order to make suitable studies, a simple fumed silica support (similar to the **MCM-41** but not containing the mesopores, neither containing the dye) functionalised with the imidazolium binding sites was prepared. This material was readily obtained by reaction of the N-methyl-N'-propyltrimethoxysilylimidazolium chloride derivative in fumed silica in acetonitrile at room temperature (solid **FS-Im**). Solid **FS-Im** was characterized by using conventional solid state techniques. The imidazolium content was determined by thermogravimetric and elemental analysis. The molar ratio between imidazolium binding molecule and  $\text{SiO}_2$  was  $5.3 \times 10^{-2}$  (0.67 mmol /g solid) that results in a relatively dense monolayer of imidazolium cations with an average distance between neighbouring imidazolium groups of ca. 10 Å. In this prepared solid the counterions of the imidazolium groups were chloride anions and we use this **FS-Im** support to study the interaction with two different guests: octanoate and dodecanoate. For this purpose, aqueous suspensions of the **FS-Im** solid were titrated with these two carboxylates and the titration followed by conductimetry. Figure I shows the conductivity of the solution as a function of the number of equivalents of carboxylate added (equivalents with respect to the equivalents of imidazolium groups in the solid; i.e. 0.67 mmol /g solid). From these titration profiles it can be seen that a large change in conductivity is observed for both carboxylates at 1 equivalent of carboxylate added. The results undoubtedly show that in both cases, for octanoate and dodecanoate, a monolayer of carboxylates coordinated to the imidazolium functionalised surface is formed. By extrapolating this result to the solid **MS-Im** it seems clear that both carboxylates coordinate on the imidazolium surface at the pore boundaries and in both cases the substitution of chloride by the corresponding carboxylate would surely be complete as it is in the **FS-Im** solid. This means that the difference observed for dodecanoate and octanoate (see Figure 2 in the manuscript) is not just because different densities of the MS-Im-carboxylate exist at the pore outlets, but most likely due to the “gate-like” effect.

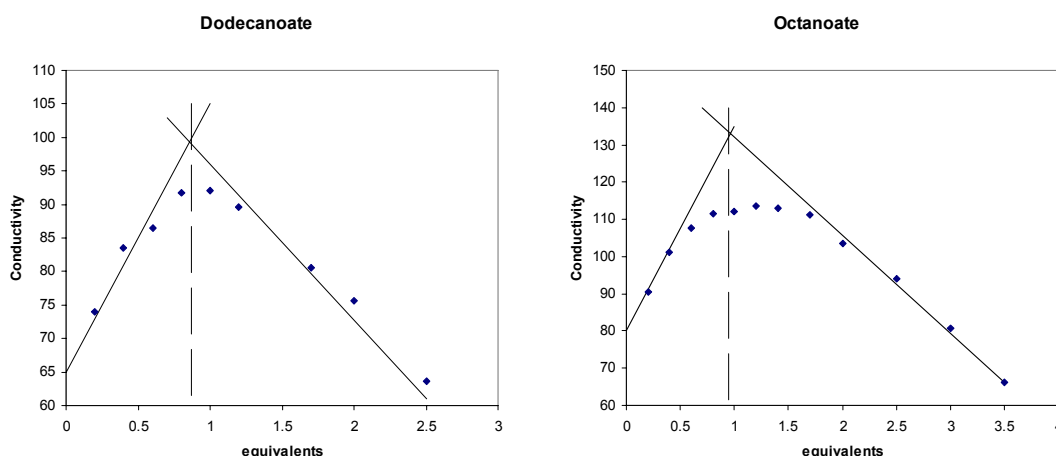


**Figure I.** Conductivity versus equivalents of carboxylate added in titration experiments of solid **FS-Im** with dodecanoate and octanoate.

### Colorimetric recognition/sensing of long-chain carboxylates

Long-chain carboxylates (the anions of fatty acids) are ubiquitous chemical compounds that play outstanding roles in many different areas that concern life at various levels. For instance the presence of long-chain carboxylates in industrial products, as indicators in biochemistry, etc makes the preparation of sensor molecules with the ability to discriminate long-chain from other carboxylates a subject of interest. Searching in the literature it is apparent that sensor molecules for short-chain mono- or dicarboxylates are abundant. However colorimetric sensors for long-chain carboxylates are very scarce.

Anion recognition studies were carried out using 10 mg of solid **MS-Im** suspended in 25 ml of aqueous solutions (buffered at pH 7.0 with HEPES,  $10^{-3}$  mol dm $^{-3}$ ) containing the corresponding anion ( $C = 10^{-3}$  mol dm $^{-3}$ ). The suspension was stirred for ca. 60 minutes to allow maximum dye delivery (see below) and then filtered-off using a teflon filter. The release of the Ru(bipy) $_3^{2+}$  dye from the pore voids to the aqueous solution was monitored via the spin allowed d- $\pi$  metal-to-ligand charge transfer (MLCT) transition band of the Ru(bipy) $_3^{2+}$  dye centred at 454 nm. In preliminary results it was found similar selectivity patterns in relation to carboxylates in the 5-8 pH range (lower pHs were not studied because protonation of the carboxylic groups, whereas higher pH values were avoided because possible OH $^-$  attack to the silica matrix). Neutral pH was finally selected for the study of sensing procedures. The **MS-Im** solid was designed to assess the possibility of using hybrid gate-like scaffoldings for sensing procedures and a set of linear carboxylates were used for testing purposes. The carboxylates of formula CH $_3$ -(CH $_2$ ) $_n$ -COO $^-$  (with  $n = 0, 2, 4, 6, 8$  and 10) were used. Longer carboxylates showed solubility problems in water at neutral pH and were not studied. The manuscript Figure 2 shows the selective response to the long-chain carboxylates decanoate and dodecanoate for which the solutions in contact with the **MS-Im** solid remained basically colourless as consequence of an effective pore blockage. In contrast, in the presence of smaller carboxylates the solid **MS-Im** displayed no sensing characteristics. A remarkable ON-OFF behaviour was observed for instance when one compares the dye delivery process in the presence of dodecanoate or octanoate. As additional complementary information Figure II shows the release kinetics observed for dye delivery from **MS-Im** in water at neutral pH in the presence of these two carboxylates ( $C_{\text{carboxylate}} = 6 \times 10^{-4}$  mol dm $^{-3}$ ). As it can be seen in this figure there is a remarkable different dye delivery process. It also can be observed that maximum dye liberation is found after ca. 40 minutes. Similar kinetic releases (not shown) to that of octanoate were found for the **MS-Im** solid alone and in the presence of shorter carboxylates such as acetate, butanoate and hexanoate. Figure III shows the absorption spectra of the dye delivered from the **MS-Im** solid in the presence of octanoate and dodecanoate solutions ( $C_{\text{carboxylate}} = 6 \times 10^{-4}$  mol dm $^{-3}$ ).

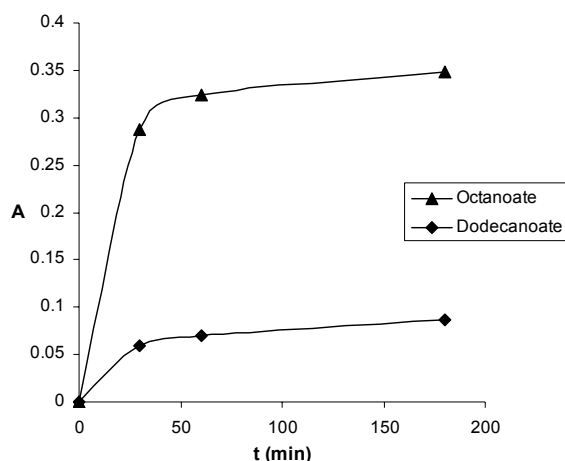


**Figure II.** Dye release kinetic for solid **MS-Im** in water (buffered at pH 7.0 with HEPES,  $10^{-3}$  mol dm $^{-3}$ ) in the presence of these octanoate or dodecanoate ( $C_{\text{carboxylate}} = 1 \times 10^{-3}$  mol dm $^{-3}$ ).

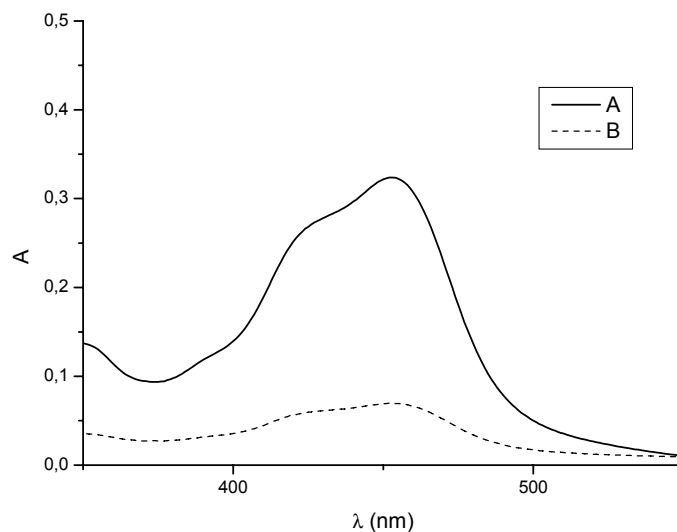


**Figure III.** Absorption spectra of the dye delivered from the **MS-Im** solid in the presence of (A) octanoate and (B) dodecanoate solutions ( $C_{\text{carboxylate}} = 1 \times 10^{-3}$  mol dm $^{-3}$ ).

Also in preliminary results dye delivery from the **MS-Im** solid was tested in the presence of other anions and cations (chloride, bromide, carbonate, nitrate, sulphate, phosphate, sodium, potassium and calcium). None of these ions act as “molecular tap” and in all cases massive dye release is observed.

As a control solid, the sensing ability of solid **FS-Im** (consisting of a “flat” surface without the presence of nanoscopic pores) was also tested under similar experimental conditions. This solid showed poorly sensing ability, i. e. the presence of octanoate induced massive dye delivery whereas in the presence of dodecanoate a minimal inhibition of  $\text{Ru}(\text{bipy})_3^{2+}$  dye delivery was observed.

Finally, and in order to test the effect exerted by carboxylates in the visible band of the dye, the changes in the spectra of  $\text{Ru}(\text{bipy})_3^{2+}$  dye in aqueous solutions (buffered at pH 7.0 with HEPES,  $10^{-3}$  mol dm $^{-3}$ ) in the presence of octanoate and dodecanoate ( $10^{-3}$  mol dm $^{-3}$ ) were measured. The changes in the visible band were negligible in the presence of both carboxylates indicating that the difference observed in the absorption spectra showed in Figure III was clearly ascribed to the gate-like mechanism proposed.